Computation of Current Distribution in YBCO Tapes With Defects Obtained From Hall Magnetic Mapping by Inverse Problem Solution

M. Carrera, J. Amorós, X. Granados, R. Maynou, T. Puig, and X. Obradors

***Abstract*—The development of superconducting devices based on long-length HTS tapes often requires of these tapes high homogeneity along its length as well as across its width. This implies the absence of significant local defects.**

Non-destructive characterization techniques to examine critical current distribution for defect detection are of great interest, specially if they could be applied in situ for real-time testing of large lengths of tape.

In this work, we continue the adaptation of our method for the computation of critical current maps from Hall measurements of the magnetic field over the tape. We compute the current density distribution in a stretch of a commercial YBCO tape which contains defects by using a specifically designed fast inverse problem solver. The 2-dimensional current map meshes with the current distributions in a cross-section of the tape that we previously computed in real time, so that a map of the critical current circulating on the entire surface of a tape with isolated defects may be obtained, regardless of its length, by running a Hall probe over it.

This method is applied to a series of Hall mappings corresponding to several magnetization regimes, produced by applying different current intensities to the tape. Details of the experiments and the calculation method are reported and the applicability to detect the impact of the defects in the tape over the current distribution is discussed.

***Index Terms*—Hall mapping, HTS tapes fast characterization, magnetic inverse calculation.**

I. Introduction

THE evolution of the increasing demand of superconducting materials, specifically superconducting tape, at the commercial level for the amount of devices that are projected or worldwide ongoing, requires large scale production and well defined quality classification to match the designers' needs. On site precise characterization is a helpful and necessary instrument which allows a better classification, homogenizing the properties of the material in each class. Identification of defects or quality fluctuations at the production level is a way for diminishing production cost and giving a confident basis for HTS device design.

Although a good characterization should include many other aspects as mechanical, thermal and magnetic behavior, at room temperature (RT) and at operating temperature (OT) several ways have been proposed for characterization of electrical properties on the basis of the magnetic and transport properties of HTS tapes including direct transport critical current ($\mathrm{I_c}$) determination in consecutive tape segments [1], mutual inductance critical current determination in an overlapped sequence [2], magnetic field trapped analysis by exploring a line of the superconducting surface after local or full magnetization [3], [4], or, finally, full Hall probe mapping [5], [6].

All the "in situ" characterization systems require giving their results in real time to get a useful feedback for the production systems. This constrain leads to both fast data collection and fast computation time to get on-the-fly availability of useful data, thus pressing for optimization of the number of points and direct identification of defects in the cached map transporting the identification process to a secondary effort done separately.

The effort of our work has been devoted to have an efficient and fast way for data collecting with high resolution and to design a fast inversion way for local $\mathrm{I_c}$ calculation from mapping of the out of plane magnetic field component. In this work we will report on the results of computation of the current distribution in a set of samples by a fast and efficient inversion method capable of reliable on-the-fly computation, as adaptation of the previously reported algorithms developed for HTS bulks [5], [7]–[9] in a first step, and extended to tapes in a second step [10].

II. Computation Model

The procedure used to invert the Biot-Savart problem on the measured tapes is an adaptation of the discretization and QR-inversion method used by the authors on bulk samples in [7]–[9].

The method is based in the subdivision of a region containing the stretch of tape to be studied into a rectangular discretization grid. The current J circulating on this region is the curl of the magnetization M, which is assumed to have a constant value $\mathrm{M_{ij}}$ on every element Δ_{ij} in this grid. If the vertical magnetic field

Manuscript received August 02, 2010; accepted October 12, 2010. Date of publication November 11, 2010; date of current version May 27, 2011. This work was supported by the Consolider NANOSELECT project funded by the Education Ministry of the Spanish Government and EU-FP7-ECCOFLOW project.

M. Carrera is with the Departament de Medi Ambient i Ciències del Sòl, Universitat de Lleida, Jaume II, 69. 25001 Lleida, Spain (e-mail: mcarrera@macs.udl.cat).

X. Granados, T. Puig, and X. Obradors are with the Institut de Ciència de Materials de Barcelona, CSIC, Campus UAB, 08193, Bellaterra, Spain (e-mail: granados@icmab.es; teresa@icmab.es; obradors@icmab.es).

J. Amorós is with the Departament de Matemàtica Aplicada I, Universitat Politècnica de Catalunya, Diagonal 647, Barcelona, Spain (e-mail: jaume.amoros@upc.edu).

R. Maynou is with CEIB-EUETIB and Departament de Matemàtica Aplicada III, Universitat Politècnica de Catalunya, Comte d'Urgell 168, Barcelona, Spain (e-mail: roger.maynou@upc.edu).

Color versions of one or more of the figures in this paper are available online at http://ieeexplore.ieee.org.

Digital Object Identifier 10.1109/TASC.2010.2089596

generated by the current is measured at a second rectangular grid of points $\mathrm{P_{kl}} = (\mathrm{x_b}, \mathrm{y_b}, \mathrm{z_b})$, at a fixed height over the tape, the magnetization values $\mathrm{M_{ij}}$ must satisfy a linear system of equations formed by an equation of the form (1) for each point $\mathrm{P_{kl}}$. In that equation r is the distance $\|\mathrm{P_{kl}} - (\mathrm{x,y,z})\|$ from the measurement point to points (x, y, z) in the element Δ_{ij}. This linear system may be duly inverted, yielding the value of its unknowns $\mathrm{M_{ij}}$.

$$B_z(P_{kl}) = \sum_{\Delta_{ij}} \left(\frac{\mu_0}{4\pi} \iint_{\Delta_{ij}} \frac{3(z_b - z)^2 - r^2}{r^5} dxdy \right) M_{ij} \quad (1)$$

In practice, to minimize the propagation of errors from the measured $\mathrm{B_z}$ to the inverted M it is advisable to measure the vertical magnetic field as closely (in all dimensions) to the tape as possible, and to take redundant measurements and solve an overdetermined linear system.

Unlike in the previous applications of this procedure to bulks, this inversion procedure is applied here to open circuits, usually to a short stretch in a long tape with current flowing in and out of the measured region. This difficulty is overcome by adding to the discretization grid a set of long, thin elements on each end of the measured stretch of tape, supporting a current that is rectilinear and homogeneous along the length of tape that they cover. The current on these tape ends is allowed to vary in intensity across the tape width to match the ends of the central discretization grid. If the actual current in these end regions is rectilinear and length-homogeneous then the 2-dimensional map for M and the circulating current density J computed in the central discretization grid is valid. If the current circulating on the ends of the tape is not rectilinear, or just unknown, the computed maps of M and J in the central discretization grid are still valid at a distance away from the ends of the grid. The safety distance is determined by the bounds on the current density, or on the irregularity of the tape, available for the tape stretches adjoining the computation region.

As the current J is the curl of the magnetization M only in closed circuits, if the tape is transporting current two lateral elements are added to the sides of the discretization grid and its ends. These elements simulate thin wires closing the circuit, and have no appreciable effect on the computation provided that they are placed symmetrically and far away from the tape.

III. YBCO Tapes

Two samples of YBCO coated conductors of different commercial suppliers have been tested:

(a) A tape with a cross width of 4.15 mm (S1). It is coated by an YBCO superconducting layer in the range of 1 μm-thickness. A metallic stabilizer made of silver and copper is coating the HTS layer with a thickness of about 25 μm over the HTS coating which separates the external explored area from the superconducting sheet.

(b) A second sample (S2) from a different supplier has also been studied. The sample with an YBCO superconducting layer in the range of one micron is protected by a metallic sheet which separates the exploring area from the HTS coating a distance in the range of 60 μm. Both magnetic contributions, that of the protecting metallic sheet and that of the substrate are negligible.

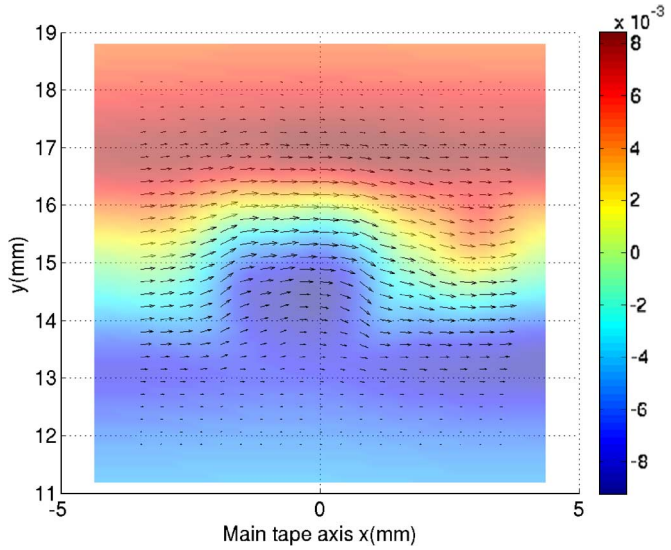

Fig. 1. Magnetic field $\mathrm{B_z(G)}$ (indicated by color) measured over a stretch of tape S1 while carrying a current of $\mathrm{I} = 85$ A after achieving its critical current of 91 A. The computed currents are shown as vector fields over the map of $\mathrm{B_z}$.

Stretches of about 7 and 12 cm of both tapes were inserted in a transport current circuit by fixing the beginning and end of the tape to blocks of Cu large enough to drain the heat produced in the contacts during the experiment. The explored area of the tapes is more than 1 cm far from the contacts for sample S1, and 2 cm in case of S2. The tapes were then immersed in liquid $\mathrm{N_2}$ at 77 K, and the circuit was designed so that the current outside the tape was symmetrically distributed on both sides of the tape so as to avoid its magnetic influence.

The tape was subjected to a ZFC process, and a transport current was applied then to the circuit, with total intensity varying from zero to critical superconducting intensity $\mathrm{I_c}$ in each tape according to the 1 $\mu\mathrm{V/cm}$ criterion. Then, the intensity was decreased to zero. The vertical magnetic field $\mathrm{B_z}$ was measured at different intensities throughout this cycle.

A Hall probe was rastered in parallel rows, crossing the tape orthogonally to its main axis, at a height of 80 μm above the tape, i.e. 100 and 150 μm (S1 and S2 respectively) above the superconducting layer. The probe had an active area of 100×100 μm, and the vertical magnetic field $\mathrm{B_z}$ above the tape was measured on each row with a steps of 50 μm.

A. Results in Tape S1

The tape S1 was object of a complete study of the distributions of field $\mathrm{B_z}$ and the current distributions obtained from inversion, corresponding to different values of applied current intensity, and showing a notably homogeneous distribution along the tape, with a critical current of 122 A. This study was reported in [10]. After this characterization, the authors have created in the tape artificial defects in different positions by puncturing it with a fine needle in order to study its influence on the current distribution.

The magnetic field $\mathrm{B_z}$ was measured on a 0.2×0.2 mm^2 grid covering a 30×30 mm^2 square over the artificial defects on the tape. Fig. 1 shows the measured magnetic field when the

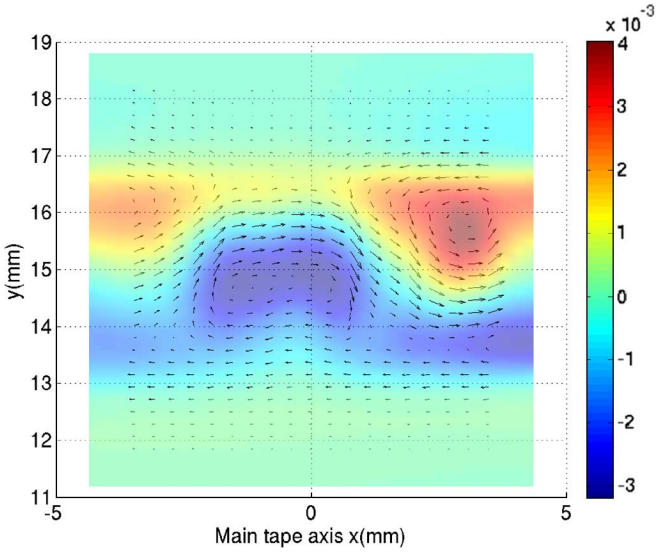

Fig. 2. Magnetic field $B_z(G)$ (indicated by color) measured over a stretch of tape S1 in state of remanence at the end of current cycle after achieving its critical current of 91 A. Computed currents are shown as vector fields over the map. of B_z.

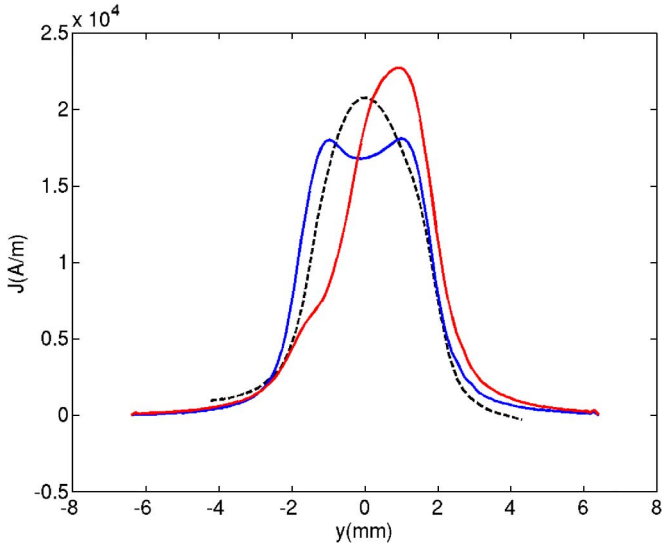

Fig. 3. Calculated current density in a transverse section of tape S1: initial sample before perturbing the tape (black, dotted line), and after holing the tape: (a) in a nonperturbed stretch (blue, continuous line, double peak), (b) across the hole (red, continuous line, single peak). In both cases the tape was submitted to the same process of carrying current (see text).

intensity of current carrying through the tape is of 85 A (after having reached its critical current at 91 A). The measurement is centered on a stretch of tape centered in the main puncture. The distribution of the current density J obtained applying our algorithm of inversion is represented as a vector field superimposed on the map of B_z of the Fig. 1, where we can observe the perturbation induced by the defect. The effect of the puncture can be seen along the axis stretch from $x = -2$ to 0.5 mm. The transport current becomes asymmetrical as most of it passes through one side of the puncture. It is likely that the current drops to zero on the puncture proper, but our discretization procedure blurs the current map on a band of 1–2 discretization elements wide around any domain, so in the case of a small perturbation like this it is able to detect a drop in the density J and a change in its direction around the hole.

Fig. 2 shows, on the same stretch of the tape S1, the map of the trapped field once the transport current has been eliminated and therefore the superconductor reaches a remanent state of magnetization.

The computed distribution of current density J, represented as vectors over the map of field B_z, reflects faithfully the disruptions caused by the hole in the circulation of the closed loops of current. It is important to note that the remanence state reflects closely the inhomogeneities in the tape, which points towards the application of this method of characterization in reel-to-reel configurations because it means that the stretch explored with the Hall probe does not need to carry current in the moment of the scanning.

In the Fig. 3 we show the distribution of current density J obtained in cross-sections of the sample S1 when the applied current is 85 A: a profile of J that corresponds to the central position of the hole in the map of Fig. 1 (red continuous line); a profile made in a homogeneous region of the tape (blue continuous line); and a profile of J (black discontinuous line) obtained from the map of B_z measured in similar conditions ($I = 80$ A) in the sample S1 before its puncturing, when all the cross-sections along the measured stretch were practically identical. Apart from the asymmetry produced by the hole, it may be observed clearly how the distribution of J reflects the fact that, because of the decrease of the total critical current, the most homogeneous regions have not achieved their local critical current when the applied intensity reached the critical current at the punctured stretch of 91 A.

According to the framework of our inverse problem solution, we suppose that the current is flowing homogenously along the z (out of plane) coordinate. The current density so obtained is considered in a single plane being an average of the actual superconducting currents. So, this current density is not a critical current density in the conception of a critical state model. The J values can vary continuously from zero to a maximum value.

If we look to the current distribution models based on superconducting considerations, full current penetration occurs from the edges to the centre [11], [12] as the overall current increases. This phenomenon does not relate with losses or dissipation but with current distribution instead. Screening concept is then the basis of the current distribution. So, if not fully penetrated, the z-averaged current gets two maxima, one in each edge, and diminishes in the central part of the tape while, when fully penetrated, this minimum tends to disappear as shown in Fig. 3. Once the sample has carried the maximum current the penetration remains, when diminishing the current again, changing the J profile from that of a non-fully-penetrated state to a fully penetrated one, as in the dashed curve of Fig. 3.

The integral current density along the transverse section of the tape must be constant thus being the overall current the same along the tape. According to that and taking into account the inhomogeneity of the tape, full penetration situation could be achieved in some sections where the overall current has achieved the maximal non dissipative value (critical current), while the achieved value has been smaller than the critical

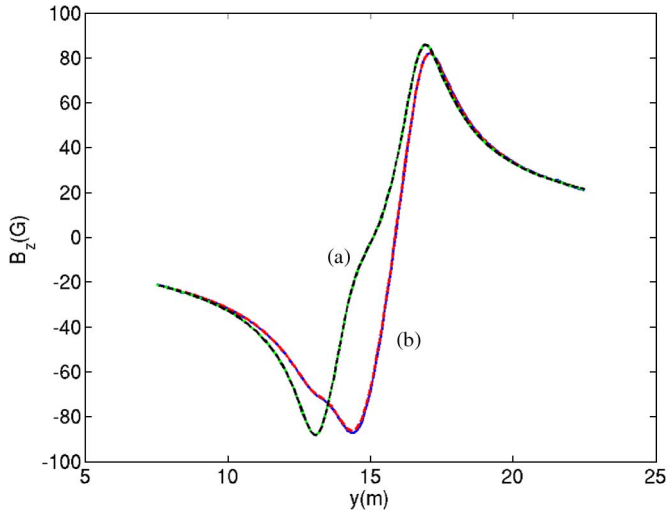

Fig. 4. Measured magnetic field $\mathrm{B_z}$ is compared to the field generated by the current determined by our computation in two cross-sections of tape S1. (a) First cross section lies in an unperturbed stretch of tape: measured $\mathrm{B_z}$ (black, dotted line) and "recomputed" $\mathrm{B_z}$ (green). (b) Second section crosses the main perturbation at $\mathrm{x} = -0.75\ \mathrm{mm}$ in the map of Fig. 2: measured $\mathrm{B_z}$ (red, dotted line) and "recomputed" $\mathrm{B_z}$ (blue).

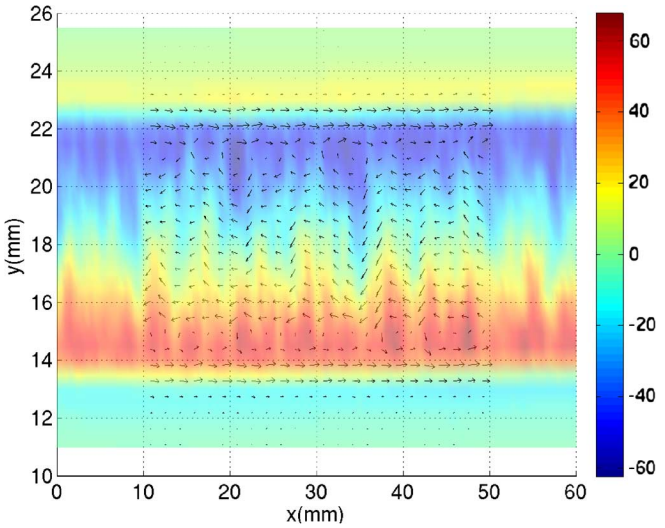

Fig. 5. Magnetic field $\mathrm{B_z(G)}$ measured over a stretch of tape S2. Computed current density is shown as a superimposed vector field. See text for details about computation process strategy.

in other sections along the magnetization process. This can be seen in the continuous curves of Fig. 3. Far away from the defect, the current profile gets the non-full-penetration shape (double peak curve) and, in the restricted section the full penetration shape (single peak) is achieved.

As an accuracy check of the inversion method, the authors computed by Biot-Savart law the magnetic field $\mathrm{B_z}$ that the distribution of current J obtained with the algorithm of inversion would produce in the grid of points used in the measure of $\mathrm{B_z}$, so that we can compare the measured field $\mathrm{B_z}$ with the recalculated field. Fig. 4 illustrates this comparison in the case of the remanence state shown in Fig. 2, taking two cross sections corresponding to the centre of the hole ($\mathrm{x} = -0.75\ \mathrm{mm}$ in the map Fig. 2), and to a homogeneous stretch of the tape. The results are typical for the application of our inversion procedure to thin tapes: the difference between the measured and recomputed field $\mathrm{B_z}$ above the tape is 3% on average, with the error concentrating over the edges.

B. Results in Tape S2

Sample S2 has been subjected to Hall probe scannings over longer tape stretches, up to 60–70 mm long, with $\mathrm{B_z}$ measured on a 30 mm wide band centered on the tape and with a resolution of $0.5 \times 0.5\ \mathrm{mm}^2$. The tape has been probed under a set of conditions ranging from a transport current bigger than its critical current of 240 A down to a remanent field state. Fig. 5 shows the magnetic field $\mathrm{B_z}$ over the tape in the remanent state at the end of the process. The distribution of the field shows that this tape is significantly inhomogeneous, unlike sample S1 before its perturbation. Therefore an accurate description of the circulating current requires 2-dimensional maps.

The computed current density J is shown in Fig. 5, as a vector field superposed to the magnetic field map. This current distribution has been obtained using a procedure apt for continuous use on tapes of any length: the current J has been computed in 3 cm-long stretches of tape (*computation windows*), based on the measured field $\mathrm{B_z}$ on each stretch and the discretization procedure for open circuits described in Section I. The result is reliable in a central stretch 1 cm-long in each computation, as it is far enough from the areas where we made any assumptions of regularity on the circulating current. The computation window has been advanced only 1 cm at a time, providing a 2 cm-long overlap with the previous window that allows for the comparison of 2 or 3 computations of J in each 1-cm stretch of tape. These computations agree, yielding the vector field plotted on Fig. 5. The vectors of current circulation J at the initial and final 1 cm-stretches of tape has not been plotted, as its computed value cannot be corroborated without knowledge of its neighboring tape areas beyond the Hall probe scan.

The resulting current distribution reflects the inhomogeneities of the superconducting tape. The current density has maximal values around 7500 A/m (corresponding to $7.5 \times 10^5\ \mathrm{A/cm}^2$ if the thickness of the HTS layer is taken into account). The fluctuation in the trapped field along the tape is detected by examining the current density on its cross sections or, more visually, by the direction of the current vectors deviating from the main tape axis.

IV. Conclusions

The work presented here shows the capability of Hall magnetometry, combined with the authors' Biot-Savart inversion procedure, for the detection of inhomogeneities in superconducting tapes and analysis of their effects.

The inversion procedure reported here allows the computation of 2-dimensional maps of current distribution in tapes with localized defects, in order to asses the impact of these defects on the current circulation and critical current level of the tape. Resolutions of up to 0.2 mm have been achieved so far in these maps.

The experimental setup employed by the authors can perform fast Hall probe measurements of $\mathrm{B_z}$ over 5–10 cm long

stretches of tape, while varying its magnetization state, and including both transport of current and remanent states. This setup can be switched to a reel-to-reel Hall probe measuring system which, combined with the above Biot-Savart inversion procedure produces in real (i.e., measuring) time 2-dimensional maps of the circulating current on a tape, regardless of its length. This real-time tape characterization scheme for long tapes will be reported elsewhere.

REFERENCES

[1] Y. Xie, H. Lee, and V. Selvamanickam Patent US2006073977-A1; WO2006036537-A2; US7554317-B2.

[2] S. Furtner, R. Nemetschek, R. Semerad, G. Sigl, and W. Prusseit, "Reel-to-reel critical current measurements of coated conductors," *Supercond. Sci. Technol.*, vol. 17, pp. S281–S284, 2004.

[3] M. Zehetmayer, M. Eisterer, and H. W. Weber, "Simulation of a current dynamics in a superconductor induced by a small permanent magnet: Application to the magnetoscan technique," *Supercond. Sci. Technol*, vol. 19, pp. S429–S437, 2006.

[4] M. Zehetmayer, R. Fuger, F. Hengstberger, M. Kitzmantel, M. Eisterer, and H. W. Weber, "Modified magnetoscan technique for assessing inhomogeneities in the current flow of coated conductors-Theory and experiment," *Physica C*, vol. 460–462, pp. 158–161, 2007.

[5] M. Carrera, X. Granados, J. Amorós, R. Maynou, T. Puig, and X. Obradors, "Detection of current distribution in bulk samples with artificial defects from inversion of Hall magnetic maps," *IEEE Trans. Appl. Supercond.*, vol. 19, no. 3, pp. 3553–3556, 2009.

[6] F. Hengstberger, M. Eisterer, M. Zehetmayer, and H. W. Weber, "Assessing the spatial and field dependence of the critical current density in YBCO bulk superconductors by scanning Hall probes," *Supercond. Sci. Technol.*, vol. 22, p. 025011, 2009, (6pp).

[7] M. Carrera, X. Granados, J. Amorós, R. Maynou, T. Puig, and X. Obradors, "Computation of critical current in artificially structured bulk samples from Hall measurements," *J. Phys.: Conf. Ser.*, vol. 97, p. 012107, 2008, (6 pp).

[8] M. Carrera, J. Amorós, A. E. Carrillo, X. Obradors, and J. Fontcuberta, "Current distribution maps in large YBCO melt-textured blocks," *Physica C*, vol. 385, pp. 539–543, 2003.

[9] M. Carrera, J. Amorós, X. Obradors, and J. Fontcuberta, "A new method of computation of current distribution maps in bulk high-temperature superconductors: Analysis and validation," *Supercond. Sci. Technol.*, vol. 16, pp. 1187–1194, 2003.

[10] M. Carrera, X. Granados, J. Amorós, R. Maynou, T. Puig, and X. Obradors, "Current distribution in HTSC tapes obtained by inverse problem calculation," *J. Phys.: Conf. Ser.*, vol. 234, p. 012009, 2010.

[11] W. T. Norris, "Calculation of hysteresis losses in hard superconductors carrying ac: Isolated conductors and edges of thin sheets," *J. Phys. D: Appl. Phys*, vol. 3, pp. 489–507, 1970.

[12] E. H. Brandt and M. Indenbom, "Type-II-superconductor strip with current in a perpendicular magnetic field," *Phys. Rev. B*, vol. 48, no. 17, pp. 12893–12906, 1993.